Dynamics of the Bose-Hubbard model: Transition from a Mott insulator to a superfluid

Fernando M. Cucchietti,[1] Bogdan Damski,[1] Jacek Dziarmaga,[2] and Wojciech H. Zurek[1]
[1]*Theory Division, Los Alamos National Laboratory, Los Alamos, New Mexico 87545, USA*
[2]*Institute of Physics and Centre for Complex Systems, Jagiellonian University, Reymonta 4, 30-059 Kraków, Poland*
(Received 15 February 2006; published 2 February 2007)

We study the dynamics of phase transitions in the one-dimensional Bose-Hubbard model. To drive the system from a Mott insulator to a superfluid phase, we change the tunneling frequency at a finite rate. We investigate the buildup of correlations during fast and slow transitions using variational wave functions, dynamical Bogoliubov theory, Kibble-Zurek mechanism, and numerical simulations. We show that time-dependent correlations satisfy characteristic scaling relations that can be measured in optical lattices filled with cold atoms.

DOI: 10.1103/PhysRevA.75.023603 PACS number(s): 03.75.Kk, 03.75.Lm

I. INTRODUCTION

The spectacular experimental realization of the Bose-Hubbard model (BHM) using cold atoms in an optical lattice [1] triggered an avalanche of both theoretical and experimental activity [2,3]. The excitement comes mostly from the fact that the derivation of the BHM in this system can be carried out rigorously [2,4], its parameters can be experimentally manipulated in real time [1], and lattice geometry can be engineered almost at will: it can be one, two, three dimensional and can have different shapes—e.g., rectangular, triangular, etc.

The physics of the Bose-Hubbard model is of both fundamental and practical interest. Indeed, the BHM is one of the model systems on which our understanding of quantum phase transitions (QPT's) is based [5,6]. The quantum phase transition happens in the BHM between the gapless superfluid (SF) phase and the gapped Mott insulator (MI) phase. Recently its signatures have been experimentally observed [1]. In a homogeneous system at fixed density, the transition takes place only when the number of atoms is commensurate with the number of lattice sites. The practical interest in the BHM originates from the possibility of the realization of a quantum computer in a system of cold atoms placed in an optical lattice [7].

In spite of experimental studies of the BHM and the large number of numerical and analytical contributions, understanding of the BHM physics is far from complete. In particular, a theory of the dynamics of the MI-SF quantum phase transition is still in its initial stages [8–11]. This is not surprising, as until very recently [8,11–15], QPT's were studied as a purely equilibrium problem. The recent progress in dynamical studies has been obtained after applying the Kibble-Zurek mechanism (KZM) [16,17], which was successful in accounting for nonequilibrium aspects of thermodynamical phase transitions [18], to the quantum case [12,14,15,19,20].

In this paper we investigate the dynamics of the one-dimensional (1D) BHM, focusing on two-point correlation functions. To describe their time dependence, we develop and use a variety of analytical approximations. We find that the two-point correlations satisfy simple characteristic scaling relations that should be experimentally measurable. Finally, we check the accuracy of our predictions with numerical simulations.

Section II presents the model and defines the quantities of interest. In Sec. III we discuss predictions coming from a toy two-site model. Section IV (V) analyzes scaling relations of correlation functions induced by fast (slow) changes of the tunneling coupling.

II. MODEL

In terms of dimensionless variables used throughout this paper, the Hamiltonian reads

$$\hat{H} = -J\sum_{i=1}^{M}(\hat{a}_{i+1}^{\dagger}\hat{a}_i + \text{H.c.}) + \frac{1}{2}\sum_{i=1}^{M}\hat{n}_i(\hat{n}_i - 1), \tag{1}$$

where we additionally assume a density of one particle per site. Such a model should be experimentally accessible in a ring-shaped optical lattice [21], where the geometry of the problem imposes periodic boundary conditions on Eq. (1). Another setup for investigations of the Bose-Hubbard model (1) will be provided by the ongoing experiment in the Raizen group [22], where a 1D homogeneous model with open boundary conditions will be realized. Below, we will assume periodic boundary conditions to minimize finite-size effects.

The Hamiltonian is driven from the MI to the SF regime by a linear ramp of the tunneling coupling

$$J(t) = \frac{t}{\tau_Q}, \tag{2}$$

where τ_Q is the quench time scale [17,23]. The evolution starts at $t=0$ from the ground state of Eq. (1)— i.e., $|1,1,\ldots\rangle$, where the numbers denote boson on-site occupations. The evolution stops at $t=\tau_Q J_{max}$, where $J_{max} \gg 1$. Therefore, the system ends up very far away from the critical point separating MI and SF phases: $J \approx 0.29$ [24]. Experimentally, the change of the tunneling coupling alone can be achieved by proper manipulation of the lattice potential amplitude, followed by adjustment of the atomic interaction strength via Feshbach resonances [25].

We are interested in the correlation functions

$$C_l(t) = \frac{1}{2}\langle\psi(t)|\hat{a}_{i+l}^{\dagger}\hat{a}_i + \text{H.c.}|\psi(t)\rangle,$$

which are directly experimentally measurable because the momentum distribution of atoms in a lattice is their Fourier transform $\sim\Sigma_l \exp(ikl)C_l$ (k is the atomic momentum) [2]. This observation shows that the correlation functions are good observables for our problem: by the end of time evolution $J \gg 1$ so that interactions between atoms are asymptotically negligible. As a result, the correlation functions take well-defined final values.

III. DYNAMICS OF TWO-SITE BOSE-HUBBARD MODEL

In this section we consider a toy two-site model, a problem that can be completely solved analytically. The results of this section will be useful later for studies of larger systems. Using symmetries of the Hamiltonian, one can show that the evolution starting from the uniform "Mott" state $|1,1\rangle$ leads to

$$|\psi(t)\rangle = a(t)|1,1\rangle + b(t)\frac{|2,0\rangle + |0,2\rangle}{\sqrt{2}}, \tag{3}$$

where $|a|^2+|b|^2=1$ and

$$i\frac{\partial}{\partial t}\begin{pmatrix} a \\ b \end{pmatrix} = \begin{pmatrix} 0 & -2\dfrac{t}{\tau_Q} \\ -2\dfrac{t}{\tau_Q} & 1 \end{pmatrix}\begin{pmatrix} a \\ b \end{pmatrix}. \tag{4}$$

A change of basis

$$(a',b') = e^{it/2}(a-b,-a-b)/\sqrt{2} \tag{5}$$

yields

$$i\frac{\partial}{\partial t}\begin{pmatrix} a' \\ b' \end{pmatrix} = \frac{1}{2}\begin{pmatrix} \dfrac{t}{\tau} & 1 \\ 1 & -\dfrac{t}{\tau} \end{pmatrix}\begin{pmatrix} a' \\ b' \end{pmatrix}, \quad \tau = \frac{\tau_Q}{4}. \tag{6}$$

This is exactly the Landau-Zener (LZ) model [26], whose relevance for the dynamics of QPT's was recently shown in Refs. [12,14,15,19,20]. The quantity of interest is $C_1(t) = 2|b'(t)|^2 - 1$, where $b'(t)$ is provided by the exact solution of the Landau-Zener model in the case when the system starts its time evolution from the ground state at $t=0$—i.e., from the anticrossing center [19,20]. This solution is a superposition of Weber functions (see Appendix of Ref. [20]), and it leads to

$$C_1(\infty) = -1 + \frac{4}{\pi\tau}\sinh\left(\frac{\pi\tau}{4}\right)e^{-\pi\tau/8}\left|\Gamma\left(1+\frac{i\tau}{8}\right) + e^{i\pi/4}\sqrt{\frac{\tau}{8}}\Gamma\left(\frac{1}{2}+\frac{i\tau}{8}\right)\right|^2, \tag{7}$$

which has the following small-τ_Q (fast quench) expansion:

$$C_1(\infty) = \frac{\sqrt{\pi}}{4}\sqrt{\tau_Q} + O(\tau_Q^{3/2}). \tag{8}$$

For large τ_Q (slow quench), we expand the gamma functions for large absolute values of the argument [27],

$$\Gamma(z) = \sqrt{2\pi}z^{z-1/2}e^{z}\left(1 + \frac{1}{12z} + \frac{1}{288z^2} + O(z^{-3})\right),$$

and use that

$$|\Gamma(ix)|^2 = \frac{\pi}{x\sinh(\pi x)},$$

$$\left|\Gamma\left(\frac{1}{2}+ix\right)\right|^2 = \frac{\pi}{\cosh(\pi x)},$$

$$\left(\frac{1+ix}{\frac{1}{2}-ix}\right)^{ix} \underset{x\to\infty}{\to} e^{-\pi x+3/2+3i/8x-3/8x^2},$$

to obtain

$$C_1(\infty) = 1 - \frac{8}{\tau_Q^2} + O(\tau_Q^{-4}). \tag{9}$$

Equation (9) is surprising since $C_1(\infty)=1-2p_{ex}$, with p_{ex} the excitation probability of the LZ system (6) at $t=\infty$. Indeed, it implies that the excitation probability equals

$$p_{ex}(t{:}0 \to \infty) = \frac{4}{\tau_Q^2}$$

when the LZ system (6) starts its evolution from the ground state at the anticrossing center ($t=0$) and evolves slowly until $t=\infty$, while it is *exponentially* small (assuming $\tau_Q \gg 1$),

$$p_{ex}(t{:}-\infty \to \infty) = \exp\left(-\frac{\pi\tau_Q}{8}\right),$$

for the LZ model evolving from $t=-\infty$ to $t=\infty$.

We have verified numerically that a slightly larger system (four atoms in four lattice sites) exhibits the same scaling of $C_1(+\infty)$ in the fast and slow transition limits. Thus, these characteristics are not specific to a two-site toy system only. In the following sections we will use different techniques to argue that the same scaling properties are shared by large lattice models.

Before proceeding further, however, we mention that the power-law behavior of the excitation probability when the evolution starts at the anticrossing can be relevant for quantum adiabatic algorithms [28]. Indeed, by starting (or, by symmetry [20], ending) the algorithm near the anticrossing center, the computation has a much higher failure probability. Thus, such situations have to be fiercely avoided when designing a path in Hamiltonian space between the initial and solution Hamiltonians.

IV. FAST TRANSITIONS

In this section we consider systems undergoing fast ($\tau_Q \ll 1$) quenches. Let us start by summarizing some relevant

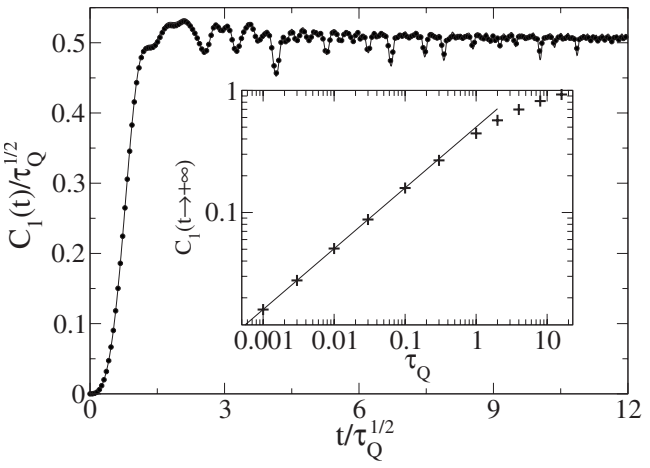

FIG. 1. Scaling properties of the first correlation function obtained numerically. Solid line: $\tau_Q=0.001$. Dots: $\tau_Q=0.03$. Inset: solid line is a power-law fit to data for $0.001 \leq \tau_Q \leq 0.1$ giving $C_1(\infty)=(0.501\pm0.005)\tau_Q^{0.498\pm0.002}$. All data are for $M=10$ and $J_{max}=600$.

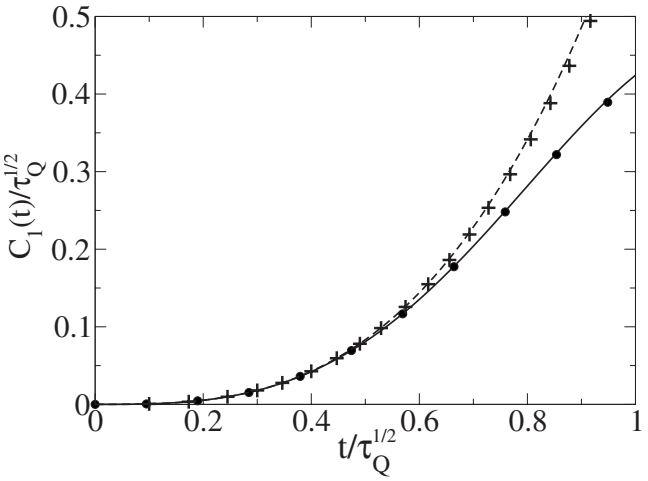

FIG. 2. Short-time dynamics of the first correlation function. The numerics for $M=10$ and $J_{max}=600$ is given by the solid line ($\tau_Q=0.001$) and large dots ($\tau_Q=0.1$). The dashed line is the variational approach, Eq. (13). The pluses (+) stand for a numerical solution of the Bogoliubov model for $\tau_Q=0.001$ and prediction (24) for $l=0$ (both data overlap).

numerical findings on C_1. We studied numerically system sizes $M=3,\ldots,10$ (M is the number of lattice sites and atoms) and found that in all cases [29]

$$C_1(\infty) = \alpha \tau_Q^{\beta} \tag{10}$$

for τ_Q's smaller than about 10^{-1}. Depending on the system size, $\alpha \in (0.37, 0.5)$, while β equals $1/2$ within fitting errors: see the inset of Fig. 1 for the $M=10$ case.

Moreover, as depicted in Fig. 1, the whole $C_1(t)$ function after the rescaling

$$C_1(t) \to \frac{C_1\left(\frac{t}{\sqrt{\tau_Q}}\right)}{\sqrt{\tau_Q}} \tag{11}$$

takes a universal form for τ_Q smaller than about 10^{-1}.

Two remarks are in order now. First, the two-site prediction, Eq. (8), shares the same scaling with τ_Q and a prefactor of the same order of magnitude ($\sqrt{\pi}/4 \approx 0.44$) as the numerics for larger systems. Second, it is interesting to ask whether the scaling relation (10) can be experimentally verified. Taking 10^{-1} as the largest τ_Q for which Eq. (10) works very well, we get $C_1(\infty) \approx 0.16$ in the $M=10$ case (Fig. 1). This is to be compared to the ground-state predictions at (i) the critical point ($C_1 \approx 0.8$ [30]) and (ii) the asymptotic value deep in superfluid ($C_1=1$). Thus, our results suggest that, despite the fast drive of the system through the transition point, the first correlation builds up macroscopically. Therefore it should be experimentally measurable in a low-temperature regime where our zero-temperature approximation is justified.

In the following we will explain the observed behavior of C_1 first by time-dependent perturbation theory and then by developing a bosonic Bogoliubov theory.

A. Short-time diabatic dynamics

For short times we can approximate the wave function using time-dependent perturbation theory,

$$|\psi(t)\rangle = a(t)|1,1,\ldots\rangle + b(t)(|0,2,1,\ldots\rangle + |2,0,1,\ldots\rangle + |1,0,2,1,\ldots\rangle + |1,2,0,1,\ldots\rangle + \cdots)/\sqrt{2M}, \tag{12}$$

where $M>2$ is assumed and $|a|^2+|b|^2=1$. A time-dependent variational principle predicts in this case that the dynamics of $a(t), b(t)$ is governed by Eq. (4) with τ_Q replaced by $\tau_Q/\sqrt{M}$. Therefore, the familiar LZ problem shows up again, and it is useful to define new amplitudes a' and b' in the same way as in Eq. (5). The dynamics of $a'(t)$ and $b'(t)$ is governed by Eq. (6) with $\tau \to \tau/\sqrt{M}$.

To describe the buildup of

$$C_1(t) = [2|b'(t)|^2 - 1]/\sqrt{M}$$

for the wave function (12), we expand the exact solution of $b'(t)$ [20] for small τ_Q, obtaining, in the lowest order,

$$\frac{C_1(t)}{\sqrt{\tau_Q}} = \frac{2}{3}\left[\frac{t}{\sqrt{\tau_Q}}\right]^3. \tag{13}$$

Expression (13) is interesting: it implies that the way in which the first correlation builds up over time is independent of system size and takes some universal (independent of τ_Q) form after simple rescalings. In Fig. 2 this prediction is compared to the numerical solution of the ten-site Hubbard model. A perfect agreement is found for times smaller than about $\frac{1}{2}\sqrt{\tau_Q}$. As will be explained in Sec. IV B, the number fluctuations start to develop significantly around $t \sim \sqrt{\tau_Q}$, so it is not surprising that a simple wave function (12) fails to describe subsequent dynamics.

B. Bogoliubov theory

Using the insight gained from the above studies, we develop a Bogoliubov approach that includes a macroscopic

number of excitations into the wave function and is able to describe longer than nearest-neighbor correlations. Our approach is a variant of the theory developed by Altman and Auerbach [11] for a large density of particles.

We truncate the Hilbert space to states with only $\{0,1,2\}$ particles per site. The initial state is the Mott state with exactly one particle per site. In a fast transition, $\tau_Q \ll 1$, we can get well into the superfluid regime of $J \gg 1$ before any substantial number fluctuations build up around the initial Mott state. Thus, in a fast transition the truncation remains valid well in the superfluid regime.

As already mentioned, the correlators C_l are conserved by the hopping term in the Hamiltonian. The hopping term dominates when $J \gg 1$, and this is why in this regime the correlators are observed to be more or less constant; see Fig. 1. Our idea is to use a truncated theory to predict the correlators $C_l(t)$ up to an instant $\tilde{t}$ so large that $J(\tilde{t}) \gg 1$, but small enough to keep the number fluctuations negligible. The predicted correlators do not change in the following evolution dominated by the hopping term, so that $C_l(\tilde{t}) \approx C_l(\infty)$.

In the truncated Hilbert space we call two particles in a site a quasiparticle and an empty site is called a quasihole. The Mott state with one particle in each site is now the "empty" vacuum state. We introduce the quasiparticle and quasihole creation operators as $\hat{c}_i^\dagger$ and $\hat{d}_i^\dagger$, respectively. Their action is best illustrated by mapping the boson occupation number onto two numbers (n_c,n_d), where n_c (n_d) are quasiparticle (quasihole) occupation numbers. This way we have in each site $|2\rangle = |(1,0)\rangle$, $|1\rangle = |(0,0)\rangle$, and $|0\rangle = |(0,1)\rangle$. Since within the $\{0,1,2\}$ subspace we cannot have two quasiparticles or holes in the same site, the hard-core constraint has to be implemented: $(\hat{c}_i^\dagger)^2 \equiv 0$ and $(\hat{d}_i^\dagger)^2 \equiv 0$. All this leads to $\hat{c}_i |\ldots,(n_c,n_d)_i,\ldots\rangle = \delta_{1n_c} |\ldots,(n_c-1,n_d)_i,\ldots\rangle$, $\hat{c}_i^\dagger |\ldots,(n_c,n_d)_i,\ldots\rangle = \delta_{0n_c} |\ldots,(n_c+1,n_d)_i,\ldots\rangle$, and analog relations for the action of $\hat{d}_i$ and $\hat{d}_i^\dagger$. Additionally, we have to remove the states with one quasiparticle and quasihole in the same site, $|\ldots,(1,1)_i,\ldots\rangle$, since these states also do not map onto the $\{0,1,2\}$ subspace. This is done by the projector $\hat{P} = \Pi_i (1 - \hat{c}_i^\dagger \hat{c}_i \hat{d}_i^\dagger \hat{d}_i)$. Finally, we note that since we deal with hard-core *bosons* all the commutators of quasiparticle and hole operators at different lattice sites commute.

In this new language the Hamiltonian (1) in the $\{0,1,2\}$ subspace equals exactly $\hat{P}\hat{H}_2\hat{P}$, where $\hat{H}_2$ is quadratic in quasihole and quasiparticle operators,

$$\hat{H}_2 = -J \sum_{\langle i,j \rangle} [2\hat{c}_i^\dagger \hat{c}_j + \hat{d}_i^\dagger \hat{d}_j + \sqrt{2}(\hat{d}_i \hat{c}_j + \hat{d}_i^\dagger c_j^\dagger)] + \sum_i \hat{c}_i^\dagger \hat{c}_i, \tag{14}$$

where $\langle i,j \rangle$ denotes nearest-neighbor pairs. We also mention here that the new operators satisfy periodic boundary conditions as the original bosonic operators do.

The truncated Hamiltonian $\hat{P}\hat{H}_2\hat{P}$ is exact in the $\{0,1,2\}$ subspace, but it is not quadratic in $\hat{c}$ and $\hat{d}$. In order to proceed we approximate $\hat{H} \approx \hat{H}_2$ and lift the hard-core bosonic constraint in all subsequent calculations: from now on $[\hat{c}_i, \hat{c}_j^\dagger] = \delta_{ij}$ and $[\hat{d}_i, \hat{d}_j^\dagger] = \delta_{ij}$. This way we arrive at a bosonic theory with a quadratic Hamiltonian $\hat{H}_2$ leading to solvable linearized equations of motion. The quadratic theory remains self-consistent as long as the average density of excitations [31],

$$\rho_{\mathrm{ex}} = \langle \hat{c}_i^\dagger \hat{c}_i \rangle = \langle \hat{d}_i^\dagger \hat{d}_i \rangle \ll \frac{1}{2}. \tag{15}$$

When $\rho_{\mathrm{ex}} \gtrsim \frac{1}{2}$ it is likely to find quasiparticles and quasiholes occupying the same lattice site and the constraint imposed by the projector $\hat{P}$ is violated.

We proceed by going to momentum space

$$\hat{c}_r = \frac{1}{\sqrt{M}} \sum_k \hat{c}_k e^{ikr}, \quad \hat{d}_r = \frac{1}{\sqrt{M}} \sum_k \hat{d}_k e^{ikr}.$$

To simplify the time-dependent calculations we add to the Fourier-transformed Hamiltonian two terms $\Sigma_k J(\hat{c}_k^\dagger \hat{c}_k - \hat{d}_k^\dagger \hat{d}_k)\cos k$ and $\Sigma_k \frac{1}{2}(\hat{d}_k^\dagger \hat{d}_k - \hat{c}_k^\dagger \hat{c}_k)$, which both commute with the Hamiltonian itself and therefore do not change the evolutions considered in this paper. The resulting Hamiltonian becomes

$$\hat{H}_2 = -J \sum_k \cos k [3\hat{c}_k^\dagger \hat{c}_k + 3\hat{d}_k^\dagger \hat{d}_k + 2\sqrt{2}(\hat{c}_k \hat{d}_{-k} + \mathrm{H.c.})] + \frac{1}{2} \sum_k (\hat{c}_k^\dagger \hat{c}_k + \hat{d}_k^\dagger \hat{d}_k). \tag{16}$$

It can be conveniently rewritten in the form

$$\hat{H}_2 = \sum_k [\hat{c}_k^\dagger, -\hat{d}_{-k}] \begin{bmatrix} \frac{1}{2} - 3J\cos k & -2\sqrt{2}J\cos k \\ 2\sqrt{2}J\cos k & 3J\cos k - \frac{1}{2} \end{bmatrix} \begin{bmatrix} \hat{c}_k \\ \hat{d}_{-k}^\dagger \end{bmatrix} + \sum_k \left(3J\cos k - \frac{1}{2} \right). \tag{17}$$

Below we look at a description of the time evolutions, leaving the discussion of the static properties of our theory to the Appendix. As in former sections we start the time evolution from $J=0$ and $J(t)$ is given by Eq. (2). We work in the Heisenberg picture where the system wave function (the ground state at $J=0$: $|1,1,\ldots\rangle$) is time independent while the operators evolve according to $i\frac{d}{dt}\hat{c}_k = [\hat{c}_k, \hat{H}_2]$ and $i\frac{d}{dt}\hat{d}_{-k}^\dagger = [\hat{d}_{-k}^\dagger, \hat{H}_2]$. It leads to

$$i\frac{d}{dt} \begin{bmatrix} \hat{c}_k \\ \hat{d}_{-k}^\dagger \end{bmatrix} = \begin{bmatrix} \frac{1}{2} - 3\frac{t}{\tau_Q}\cos k & -2\sqrt{2}\frac{t}{\tau_Q}\cos k \\ 2\sqrt{2}\frac{t}{\tau_Q}\cos k & 3\frac{t}{\tau_Q}\cos k - \frac{1}{2} \end{bmatrix} \begin{bmatrix} \hat{c}_k \\ \hat{d}_{-k}^\dagger \end{bmatrix}, \tag{18}$$

which has the following general solution:

$$\hat{c}_k(t) = u_k(t)\hat{c}_k(0) + \tilde{v}_k(t)\hat{d}_{-k}^\dagger(0),$$

$$\hat{d}_{-k}^{\dagger}(t) = v_k(t)\hat{c}_k(0) + \tilde{u}_k(t)\hat{d}_{-k}^{\dagger}(0),$$

with initial conditions $u_k(0)=\tilde{u}_k(0)=1$ and $v_k(0)=\tilde{v}_k(0)=0$. After some algebra based on Eq. (18) one finds that $\tilde{v}_k=v_k^*$ and $\tilde{u}_k=u_k^*$—this simplification showed up thanks to the convenient addition of the two constants of motion to the Fourier-transformed quadratic Hamiltonian (see above). The time evolution of the modes is given by

$$i\frac{d}{dt}\begin{bmatrix} u_k \\ v_k \end{bmatrix} = \begin{bmatrix} \frac{1}{2} - 3\frac{t}{\tau_Q}\cos k & -2\sqrt{2}\frac{t}{\tau_Q}\cos k \\ 2\sqrt{2}\frac{t}{\tau_Q}\cos k & 3\frac{t}{\tau_Q}\cos k - \frac{1}{2} \end{bmatrix}\begin{bmatrix} u_k \\ v_k \end{bmatrix}. \tag{19}$$

Additionally, we see that the Bose commutation between the time-dependent operators requires that $|u_k(t)|^2-|v_k(t)|^2=1$, which is conserved by the time evolution (19). All expectation values can be calculated after solving Eq. (19) using the fact that the wave function in the Heisenberg picture is $|\Psi\rangle = |1,1,\ldots\rangle$ for all times, so that $\hat{d}_r(0)|\Psi\rangle=0$ and $\hat{c}_r(0)|\Psi\rangle=0$.

In the following we use a perturbative solution of Eq. (19) in powers of $\sqrt{\tau_Q}$. The discussion is simplified by introducing a new timelike variable

$$s = \frac{t^2}{\tau_Q}, \tag{20}$$

whose form is motivated by the scaling property (11). Equation (19) becomes

$$i\frac{d}{ds}\begin{bmatrix} u_k \\ v_k \end{bmatrix} + \cos k \begin{bmatrix} \frac{3}{2} & \sqrt{2} \\ -\sqrt{2} & -\frac{3}{2} \end{bmatrix}\begin{bmatrix} u_k \\ v_k \end{bmatrix} = \frac{\sqrt{\tau_Q}}{4\sqrt{s}}\begin{bmatrix} 1 & 0 \\ 0 & -1 \end{bmatrix}\begin{bmatrix} u_k \\ v_k \end{bmatrix}, \tag{21}$$

with $u_k(0)=1$ and $v_k(0)=0$. This equation can be solved iteratively in powers of the small parameter $\sqrt{\tau_Q}\ll 1$.

As a self-consistency check, we calculate the density of excitations, Eq. (15). Assuming a fast-transition limit, $\tau_Q \ll 1$, we solve Eqs. (21) to zero order in $\sqrt{\tau_Q}$ and find that

$$\rho_{ex} = \frac{1}{2\pi}\int_{-\pi}^{\pi} dk|v_k|^2 \approx s^2$$

for small s. Therefore, $\rho_{ex}\ll\frac{1}{2}$ for $s\ll\frac{1}{\sqrt{2}}$ so that the quadratic approximation breaks down at

$$\frac{\tilde{t}^2}{\tau_Q} \equiv \tilde{s} \simeq \frac{1}{\sqrt{2}} \tag{22}$$

or at $\tilde{t}\simeq\sqrt{\tau_Q/\sqrt{2}}$. In a linear quench (2) this breakdown time corresponds to

$$\tilde{J} \simeq \frac{1}{\sqrt{\sqrt{2}\tau_Q}} \gg 1,$$

which is well in the superfluid regime for a fast transition. Therefore, when $\tau_Q\ll 1$, our linearized Bogoliubov approach does not break down until well in the superfluid regime.

These calculations prove that the Bogoliubov approach works reliably before $\tilde{J}\gg 1$ and the correlation functions are (see the Appendix for static predictions) [32]

$$C_l = \int_{-\pi}^{\pi}\frac{dk}{2\pi}\cos(kl)\left[3|v_k|^2 + \sqrt{2}(u_k v_k^* + u_k^* v_k)\right]. \tag{23}$$

Solving Eq. (21) we find that $C_{2l}(t)=O(\tau_Q)$, while

$$\frac{C_{2l+1}(t)}{\sqrt{\tau_Q}} = \frac{8\pi s^{3/2}}{3}\sum_{n=l}^{\infty}(-1)^{n+1}\alpha_{l,n}s^{2n}, \tag{24}$$

with coefficients

$$\alpha_{l,n} = \frac{\left(\frac{3}{4}\right)_n \Gamma(2+2n)\Gamma[1-2l+2n]^{-1}\Gamma[3+2l+2n]^{-1}}{n!\left(\frac{3}{2}\right)_n\left(\frac{7}{4}\right)_n \Gamma\left[-\frac{1}{2}-l-n\right]\Gamma\left[\frac{1}{2}+l-n\right]}$$

and $(x)_n \equiv \Gamma[x+n]/\Gamma[x]$. To obtain this series expansion we differentiate $\frac{d}{ds}C_l$ in Eq. (23), remove the resulting s derivatives with the help of the equations of motion (21), keep only the leading terms $\sim\sqrt{\tau_Q}$, and finally integrate such obtained $\frac{d}{ds}C_l$ over s to get $C_l(s)$.

The first term in the $l=0$ version of Eq. (24) reproduces Eq. (13). As shown in Fig. 2, Eq. (24) works very well until $s\simeq 1/\sqrt{2}$—i.e., up to the expected breakdown of the Bogoliubov approach (22).

Since we consider $\tau_Q\ll 1$, we have $\tilde{J}=\tilde{t}/\tau_Q\gg 1$, and thus the rest of the evolution after $\tilde{J}$ is dominated by the hopping term that does not change the correlation functions. Therefore, the correlators at the break down time $\tilde{t}$ are good estimates of the final correlation function

$$C_l(\infty) \approx C_l(\tilde{t}). \tag{25}$$

Setting $s=\tilde{s}=1/\sqrt{2}$ in Eq. (24) for definiteness we get, with an accuracy of $O(\tau_Q^{3/2})$,

$$C_1(\infty) \approx 3.9\times 10^{-1}\sqrt{\tau_Q},$$

$$C_3(\infty) \approx -3.5\times 10^{-3}\sqrt{\tau_Q},$$

$$C_5(\infty) \approx 1.4\times 10^{-5}\sqrt{\tau_Q}.$$

By solving Eq. (21) perturbatively we find with an accuracy of $O(\tau_Q^2)$ that

$$C_2(\infty) \approx 4.0\times 10^{-2}\tau_Q,$$

$$C_4(\infty) \approx -3.2\times 10^{-4}\tau_Q,$$

$$C_6(\infty) \approx 1.1 \times 10^{-6} \tau_Q.$$

The first correlation $C_1(\infty)$ fits well our numerical results—compare to Eq. (10). Reliable numerical verification of longer-range correlations would require calculations done on systems larger than our $M \leq 10$. Indeed, in small-size numerics it is hard to filter out finite-size effects especially when the long-range correlations, which are small in magnitude, are considered. Nevertheless, the Bogoliubov theory and our finite-size numerics agree that correlations C_l decay fast with the distance l.

In contrast to the simple two-site toy model of Sec. III, the Bogoliubov approach is able to describe not only nearest-neighbor but also longer-range correlations. However, it turns out that in fast transitions the correlation functions are dominated by the nearest-neighbor term C_1 with other terms being relatively small, if not negligible. This explains why already the simple two-site toy model gives such surprisingly accurate predictions for larger systems in the fast-transition limit.

V. SLOW TRANSITIONS

In this section we focus on the limit of slow transitions—i.e., $\tau_Q \gg 1$. Numerical studies in this regime are extremely time consuming; therefore, we concentrate only on analytical results. Our predictions are based on the Kibble-Zurek mechanism that was successful in describing nonequilibrium thermodynamical phase transitions and apparently works for quantum phase transitions as well [12,14,15,19,20].

According to KZM, excitations of the system after a *slow* transition have the characteristic length scale [23]

$$\xi \sim \tau_Q^{\nu/(z\nu+1)}, \tag{26}$$

where z and ν are critical exponents and the quench time τ_Q is taken as $(dJ/dt)^{-1}$ at the critical point (J is the parameter driving the transition). For the Bose-Hubbard model the dynamical exponent $z=1$. The MI-SF transition (at fixed integer density of atoms) in a d-dimensional Bose-Hubbard model belongs to the universality class of a $(d+1)$-dimensional XY spin model [6]. In one dimension this mapping implies that $\nu \to \infty$ (Kosterlitz-Thouless transition). As a result, $1-C_1$, which is proportional to the hopping energy of long-wavelength excitations, should scale for $\tau_Q \gg 1$ as

$$1 - C_1(\infty) \sim \frac{1}{\xi^2} \sim \frac{1}{\tau_Q^2}. \tag{27}$$

The exponent -2 means a rather steep dependence of the hopping energy on the quench time τ_Q, which should make it easily discernible experimentally.

Using (26) and (27) it is easy to provide predictions for two- ($\nu \approx 0.67$ [33]) and three- ($\nu=1/2$ [6]) dimensional Bose-Hubbard models. In the two-dimensional case one has

$$1 - C_1(\infty) \sim \frac{1}{\tau_Q^{0.8}},$$

while in the three-dimensional model

$$1 - C_1(\infty) \sim \frac{1}{\tau_Q^{2/3}}.$$

It would be very interesting to verify scaling relations shown in this section either experimentally or numerically.

VI. SUMMARY

We described the buildup of correlations in the BHM during transitions from a Mott insulator to a superfluid regime using a variational wave function, the dynamical one-dimensional Bogoliubov theory, the Kibble-Zurek mechanism, and numerical simulations. The time-dependent correlations satisfy characteristic scaling relations that are directly experimentally measurable.

ACKNOWLEDGMENTS

This research was supported by the U.S. Department of Energy and NSA. J.D. was supported by Polish Government scientific funds and Marie Curie ToK scheme COCOS.

APPENDIX: GROUND-STATE PROPERTIES OF THE BOSE-HUBBARD MODEL WELL IN THE MOTT REGIME

Here we discuss the ground-state properties of the Bose-Hubbard model predicted by the Bogoliubov theory. The Hamiltonian (16) can be diagonalized by the Bogoliubov transformation

$$\hat{c}_k = u_k \hat{B}_k + v_k^* \hat{A}_{-k}^\dagger, \quad \hat{d}_{-k}^\dagger = v_k \hat{B}_k + u_k^* \hat{A}_{-k}^\dagger, \tag{A1}$$

where $u_k(J)$ and $v_k(J)$ determine the static properties of the Bogolubov vacuum.

Here the Bogoliubov modes (u_k, v_k) are the eigenmodes of the stationary Bogoliubov–de Gennes equations

$$\omega_k \begin{bmatrix} u_k \\ v_k \end{bmatrix} = \begin{bmatrix} -3J\cos k + \frac{1}{2} & -2\sqrt{2}J\cos k \\ 2\sqrt{2}J\cos k & 3J\cos k - \frac{1}{2} \end{bmatrix} \begin{bmatrix} u_k \\ v_k \end{bmatrix}, \tag{A2}$$

with positive norm $|u_k|^2 - |v_k|^2 = 1$ and eigenfrequency

$$\omega_k = \frac{1}{2}\sqrt{4J^2\cos^2 k - 12J\cos k + 1}.$$

The normalization condition guarantees bosonic commutation relations of $\hat{A}_k$ and $\hat{B}_k$ operators: $[\hat{A}_k, \hat{A}_p^\dagger] = [\hat{B}_k, \hat{B}_p^\dagger] = \delta_{kp}$, $[\hat{A}_k, \hat{B}_p] = 0$, etc. The diagonalized Hamiltonian

$$\hat{H}_2 = \sum_k \omega_k \left(\hat{A}_k^\dagger \hat{A}_k + \hat{B}_k^\dagger \hat{B}_k \right) + \sum_k \left(\omega_k + 3J\cos k - \frac{1}{2} \right) \tag{A3}$$

is a sum of Bogoliubov quasiparticle excitations. Its ground state is a Bogoliubov vacuum annihilated by all $\hat{A}_k$ and $\hat{B}_k$.

Now we calculate different quantities assuming that the system size $M \to \infty$. As a self-consistency check we calculate the density of excitations

$$\rho_{\mathrm{ex}} = \frac{1}{2\pi}\int_{-\pi}^{\pi} dk |v_k|^2 = 4J^2 + O(J^4). \tag{A4}$$

The density remains $\ll \frac{1}{2}$ for $J \ll \frac{1}{2\sqrt{2}}$—compare to (15).

The expression for correlation functions in the static calculations is obtained after using [32]. Due to similarity in the notation, it is the same as Eq. (23), except that now u_k and v_k depend on J rather than t. As a result we get

$$C_1 = 4J + O(J^3),$$

$$C_2 = 18J^2 + O(J^4),$$

$$C_3 = 88J^3 + O(J^5),$$

$$C_4 = 450J^4 + O(J^6),$$

$$C_5 = 2364J^5 + O(J^7),$$

$$C_6 = 12642J^6 + O(J^8),$$

$$C_7 = 68464J^7 + O(J^9).$$

These results in the *lowest* nontrivial order listed above agree perfectly with perturbative ones. Indeed, $C_1, \ldots, C_3$ can be found in Eq. (5) of [30], while $C_4, \ldots, C_7$ match unpublished results by one of us (B.D.). A discussion of this intriguing finding is beyond the scope of this study and is left out for further detailed investigations.

To close the discussion of the static properties of our theory, we notice that also the ground-state energy per site ($\mathcal{E}$), predicted by the Bogolubov theory, agrees in the lowest order with exact perturbative calculation. Indeed, we get from Eq. (A3) that

$$\mathcal{E} = \frac{1}{2\pi}\int_{-\pi}^{\pi} dk \left(\omega_k + 3J\cos k - \frac{1}{2}\right) = -4J^2 + O(J^4),$$

which has to be compared to Eq. (3) of [30].

[1] M. Greiner, O. Mandel, T. Esslinger, T. W. Hansch, and I. Bloch, Nature (London) **415**, 39 (2002).
[2] W. Zwerger, J. Opt. B: Quantum Semiclassical Opt. **5**, S9 (2003).
[3] D. Jaksch and P. Zoller, Ann. Phys. (N.Y.) **315**, 52 (2005).
[4] D. Jaksch, C. Bruder, J. I. Cirac, C. W. Gardiner, and P. Zoller, Phys. Rev. Lett. **81**, 3108 (1998).
[5] S. Sachdev, *Quantum Phase Transitions* (Cambridge University Press, Cambridge, UK, 2001).
[6] M. P. A. Fisher, P. B. Weichman, G. Grinstein, and D. S. Fisher, Phys. Rev. B **40**, 546 (1989).
[7] D. Jaksch, H. J. Briegel, J. I. Cirac, C. W. Gardiner, and P. Zoller, Phys. Rev. Lett. **82**, 1975 (1999); G. K. Brennen, C. M. Caves, P. S. Jessen, and I. H. Deutsch, *ibid.* **82**, 1060 (1999).
[8] J. Dziarmaga, A. Smerzi, W. H. Zurek, and A. R. Bishop, Phys. Rev. Lett. **88**, 167001 (2002); A. K. Tuchman, C. Orzel, A. Polkovnikov, and M. A. Kasevich, e-print cond-mat/0504762.
[9] K. Sengupta, S. Powell, and S. Sachdev, Phys. Rev. A **69**, 053616 (2004).
[10] A. Polkovnikov, S. Sachdev, and S. M. Girvin, Phys. Rev. A **66**, 053607 (2002).
[11] E. Altman and A. Auerbach, Phys. Rev. Lett. **89**, 250404 (2002).
[12] W. H. Zurek, U. Dorner, and P. Zoller, Phys. Rev. Lett. **95**, 105701 (2005).
[13] A. Polkovnikov, Phys. Rev. B **72**, 161201(R) (2005).
[14] J. Dziarmaga, Phys. Rev. Lett. **95**, 245701 (2005).
[15] R. W. Cherng and L. S. Levitov, Phys. Rev. A **73**, 043614 (2006).
[16] T. W. B. Kibble, J. Phys. A **9**, 1387 (1976); Phys. Rep. **67**, 183 (1980).
[17] W. H. Zurek, Nature (London) **317**, 505 (1985); Phys. Rep. **276**, 177 (1996).
[18] C. Bauerle *et al.*, Nature (London) **382**, 332 (1996); V. M. H. Ruutu *et al.*, *ibid.* **382**, 334 (1996); R. Carmi, E. Polturak, and G. Koren, Phys. Rev. Lett. **84**, 4966 (2000); M. J. Bowick *et al.*, Science **263**, 943 (1994); I. Chuang *et al.*, *ibid.* **251**, 1336 (1991).
[19] B. Damski, Phys. Rev. Lett. **95**, 035701 (2005).
[20] B. Damski and W. H. Zurek, Phys. Rev. A **73**, 063405 (2006).
[21] L. Amico, A. Osterloh, and F. Cataliotti, Phys. Rev. Lett. **95**, 063201 (2005).
[22] T. P. Meyrath, F. Schreck, J. L. Hanssen, C.-S. Chuu, and M. G. Raizen, Phys. Rev. A **71**, 041604(R) (2005); M. Raizen (private communication).
[23] N. D. Antunes, L. M. A. Bettencourt, and W. H. Zurek, Phys. Rev. Lett. **82**, 2824 (1999).
[24] T. D. Kühner, S. R. White, and H. Monien, Phys. Rev. B **61**, 12474 (2000).
[25] E. Timmermans, P. Tommasini, M. Hussein, and A. Kerman, Phys. Rep. **315**, 199 (1999).
[26] C. Zener, Proc. R. Soc. London, Ser. A **137**, 696 (1932).
[27] I. S. Gradshteyn and I. M. Ryzhik, *Table of Integrals Series and Products*, 4th ed. (Academic Press, New York, 1965).
[28] E. Farhi *et al.*, Science **292**, 472 (2001).
[29] We approximate in numerical calculations $C_1(\infty)$ by $C_1(t=J_{max}\tau_Q)$, which should be a reasonable assumption as long as $J_{max} \gg 1$. In our calculations $J_{max}=600$.
[30] B. Damski and J. Zakrzewski, Phys. Rev. A **74**, 043609 (2006).
[31] In our theory $\hat{c}_i^\dagger \hat{c}_i$ and $\hat{d}_i^\dagger \hat{d}_i$ are expressed in terms of bosonic number operators as $\frac{1}{2}\hat{n}_i(\hat{n}_i-1)$ and $\frac{1}{2}(\hat{n}_i-1)(\hat{n}_i-2)$, respectively. Therefore one gets $\langle \hat{c}_i^\dagger \hat{c}_i\rangle = \langle \hat{d}_i^\dagger \hat{d}_i\rangle$ as long as $\langle \hat{n}_i\rangle = 1$, which is assumed in Eq. (15).
[32] To calculate C_l one finds that within the approximations used in this paper $\hat{a}_{i+l}^\dagger \hat{a}_i \approx 2\hat{c}_{i+l}^\dagger \hat{c}_i + \hat{d}_{i+l}\hat{d}_i^\dagger + \sqrt{2}(\hat{d}_{i+l}\hat{c}_i + \hat{d}_i^\dagger \hat{c}_{i+l}^\dagger)$.
[33] M. Campostrini, M. Hasenbusch, A. Pelissetto, P. Rossi, and E. Vicari, Phys. Rev. B **63**, 214503 (2001).